

Oscillatory exchange coupling in Fe/Au/Fe(100)

J. Unguris, R. J. Celotta, and D. T. Pierce

Electron Physics Group, National Institute of Standards and Technology, Gaithersburg, Maryland 20899

Scanning electron microscopy with polarization analysis was used to investigate the interlayer exchange coupling in Fe/Au/Fe(100) sandwich structures. The films were epitaxially grown on single-crystal Fe(100) substrates. Electron diffraction measurements revealed that the Au spacer film grew with a surface reconstruction consistent with that observed for bulk Au crystals. The exchange coupling oscillates between primarily ferromagnetic and antiferromagnetic coupling for Au spacer layers up to 65 layers (13 nm) thick, but a significant biquadratic coupling component was also observed. The oscillatory coupling exhibited two components with periods of 2.48 ± 0.05 layers (0.506 ± 0.010 nm) and 8.6 ± 0.3 layers (1.75 ± 0.06 nm). The measured periods are in excellent agreement with those calculated from spanning vectors of the Au Fermi surface.

I. INTRODUCTION

Magnetic measurements from atomically well-ordered magnetic multilayer structures are essential in order to make meaningful evaluations of various models of oscillatory exchange coupling. Thickness variations due to deviations from ideal layer-by-layer growth can obscure important features of the magnetic coupling. For example, in Fe/Cr/Fe multilayers it has been shown that a Cr spacer roughness of only a quarter layer can completely obscure the short, two-layer period, exchange coupling oscillations.¹⁻³

In this work we have investigated the interlayer exchange coupling in epitaxially grown Fe/Au/Fe(100) sandwich structures. Au(100) rotated by 45° is a very close lateral match to the Fe(100) surface and should therefore be a possible candidate for atomically well-ordered growth. In previous work, where the Fe/Au/Fe multilayer was deposited on a Ag(100) substrate, Celinski and Heinrich⁴ did not observe any well-defined oscillatory behavior of the exchange coupling through the Au(100). Using GaAs(100) substrates to grow Fe(100) and a wedge-shaped Au spacer layer, Fuss *et al.*⁵ observed oscillatory coupling consisting of a long-period component of 6.9 layers and a weaker short-period oscillation of about two layers. We have used single-crystal Fe whisker substrates in our studies and have observed very well-defined short- and long-period coupling oscillations that extended over a large Au thickness range.

II. EXPERIMENT

The experimental procedures used to investigate the exchange coupling in Fe/Au/Fe have been described in detail elsewhere.^{2,6} Briefly, the chemical composition and the structural order of the samples were measured using scanning Auger spectroscopy and reflection high-energy electron diffraction (RHEED), respectively. Scanning electron microscopy with polarization analysis (SEMPA) was used to make *in situ* measurements of the sample's magnetization during and following film growth. The films were grown on Fe(100) single-crystal substrates that were cleaned by Ar-ion sputtering followed by 750°C annealing cycles. Scanning tunneling microscope images of similar whiskers show high-quality surfaces with only about one single atomic height step per square μm .⁷ RHEED patterns from the bare whiskers showed sharp diffraction spots distributed along Laue arcs as

expected for a perfect crystal. The Auger spectra established that contamination levels were below 0.05 monolayers.

In order to measure the Au thickness dependence of the exchange coupling, wedge-shaped Au spacer layers were grown by moving a shutter in front of the Fe substrate during Au deposition. The geometry of the wedge is shown schematically in Fig. 1. The slope of the Au wedge was small, about 0.001° , which is less than the 0.01° average slope of the Fe whisker substrate. Au spacer layers were grown at Fe substrate temperatures between 80 and 100°C , and at an evaporation rate of about 8 layers/min. The direction of the interlayer exchange coupling was determined by measuring the magnetization of the top Fe film with SEMPA. Fe whisker substrates with the simple two-domain structure shown in Fig. 1 were used in order to check for and eliminate any instrumental offsets in the SEMPA measurement.

III. RESULTS

The crystalline order and thickness of the Au films were measured using spatially resolved scanning RHEED. Figure 2 shows the specular RHEED intensity as the incident electron beam was scanned along the wedge and a RHEED pattern from a 10-layer-thick Au film. The RHEED intensity oscillations were used to determine the Au thickness con-

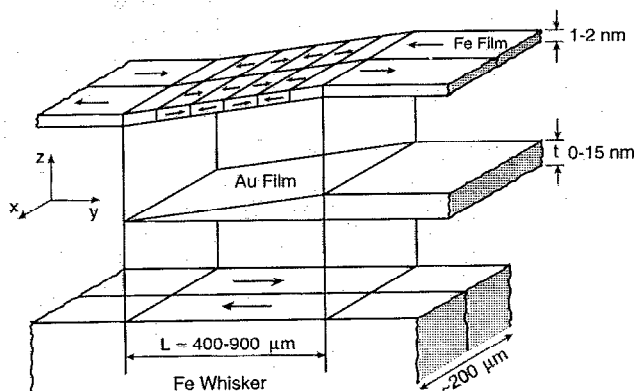


FIG. 1. An exploded schematic view of the sample structure showing the Fe(100) single-crystal whisker substrate, the evaporated Au wedge, and the Fe overlayer. Arrows in the Fe show the magnetization direction.

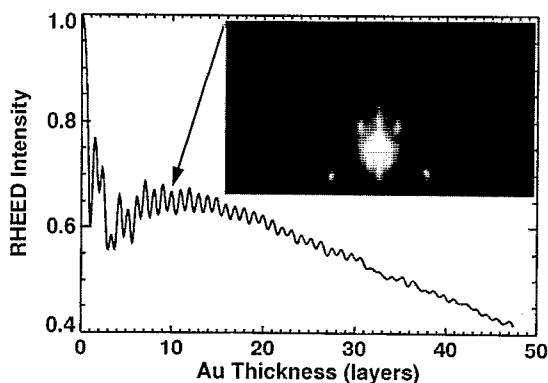


FIG. 2. The specular RHEED intensity as a function of the Au thickness obtained by scanning the electron beam along the wedge. A RHEED pattern from a 10-layer-thick film is shown in the inset.

tours along the wedge. For Au films less than three layers thick, the RHEED patterns were similar to those for clean Fe, but after three layers the diffraction spots stretched into sharp streaks and superlattice streaks began to form. The four extra streaks that appeared between the primary diffraction beams were characteristic of a fivefold surface reconstruction. Both (5×1) and (5×20) surface reconstructions have been observed for bulk Au.⁸ While the presence of streaks in the diffraction patterns indicates some disorder, the surface reconstruction suggests that the Au films have bulklike structural order. In fact the sharpness of the streaks indicates that the Au grows in patches that are internally well ordered but slightly misaligned with respect to one another.

The direction of the magnetic coupling was determined by measuring the magnetization of the top Fe film using SEMPA. A SEMPA image of a Au wedge coated with five layers of Fe is shown in Fig. 3. The component of the magnetization along the whisker direction is M_y and the orthogonal component of the in plane magnetization is M_x . Oscillations between ferromagnetic and antiferromagnetic "bilinear" coupling are most clearly visible in the M_y component. The M_x component, on the other hand, emphasizes

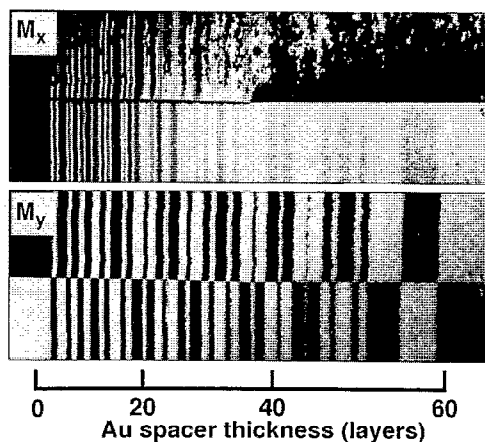


FIG. 3. SEMPA images from the five-layer-thick Fe overlayer, showing the in-plane magnetization components along the wedge, M_y , and orthogonal to the wedge, M_x .

the perpendicular "biquadratic" coupling between the Fe film and substrate. The thickness scale on these images is not linear, because of a gradual drift in the Au evaporation rate. This nonlinearity, as well as any other spatial variations in the Au thickness, was accounted for by using scanning RHEED images from the same region. The scanning RHEED images were correlated with the SEMPA images by aligning topographic features in the RHEED images with the same features in intensity images that were acquired at the same time as the magnetization images.

Averaged, linearized line scans of M_y taken from the data in Fig. 3 and from a different Fe/Au/Fe(100) wedge are shown in Fig. 4. One can see from these data that the periodicity of the coupling is very reproducible, but the amplitude of the oscillations and the thickness at which they eventually vanish vary among samples grown under slightly different conditions.

In order to measure the coupling periods precisely, we followed a previously described procedure⁶ and modeled the bilinear coupling J by the sum of two sine waves such that

$$J = A_1 \sin(2\pi t/d_1 + \phi_1) + A_2 \sin(2\pi t/d_2 + \phi_2), \quad (1)$$

where t is the Au thickness, and A , d , and ϕ are adjustable amplitudes, periods, and phases, respectively. To simulate the SEMPA data, this continuous function was first discretized with the Au lattice so that each monolayer was assigned a single coupling strength. The thicknesses at which the coupling switched sign were then determined by taking the weighted average of the coupling from adjacent layers. Finally, all positive coupling values were set to the same magnetization level and all negative coupling to the equal but opposite magnetization. Figure 4 shows the results of a calculation that gave the best fit of the model to the data. The parameter values for this model were $A_1/A_2=2.1$, $d_1=2.48$ layers, $\phi_1=0.44$, $d_2=8.60$ layers, and $\phi_2=3.14$.

In addition to the bilinear coupling, biquadratic coupling was also observed in these films. While SEMPA cannot directly measure the absolute strength of the magnetic coupling, the magnetization direction is roughly proportional to the ratio of the biquadratic to bilinear coupling.⁹ The M_x

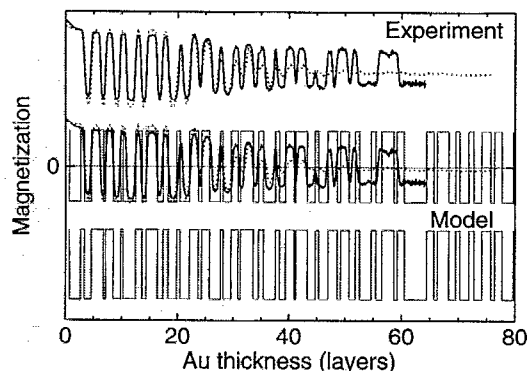


FIG. 4. The results of the model calculation described in the text are compared with an averaged, linearized line scan of the M_y data from Fig. 3 and from a SEMPA measurement from a different wedge (dotted line). For comparison, the calculated (bottom) and measured (top) curves are shown both separately and overlaid.

image in Fig. 3 shows that in the thin part of the wedge the biquadratic coupling is only significant at the transitions between the ferromagnetic and antiferromagnetic regions. As the Au thickness increases, the relative strength of the biquadratic coupling also increases, so that for thicknesses greater than about 20 layers, the biquadratic coupling is always present, and the coupling oscillations are no longer between purely ferromagnetic or antiferromagnetic states, but between some intermediate angles. For thicker Au films the coupling also tends to break up randomly into islands with different M_x magnetization components but the same M_y component. The formation of these regions is not understood, but the length scales involved suggest that it is related to the details of the Au growth.

IV. DISCUSSION

Qualitatively, the Au results are similar to SEMPA measurements of the coupling in Fe/Cr/Fe(100) (Ref. 2) and Fe/Ag/Fe(100) (Ref. 6). In each case, oscillatory coupling was observed that consisted of two periodic components, and the oscillations persisted for spacer layers greater than 10 nm thick. Another common feature of these films grown on Fe whisker substrates is that the short-period oscillations are more pronounced and the oscillations extend over a greater thickness range than in multilayers grown on more conventional substrates. Fe/Au/Fe sandwiches grown on Ag substrates show no oscillatory coupling.⁴ Fe/Au/Fe sandwiches grown on GaAs substrates only reveal weak short-period modulations in the long-period antiferromagnetic coupling.⁵

The ability to observe many coupling oscillations over a large interlayer thickness range allows the coupling periods to be measured with sufficient precision to provide a stringent test of current theories of multilayer exchange coupling. Currently, there are two quantitative predictions of Fe/Au/Fe coupling periods available. In both theories the oscillatory coupling periods are determined by wave vectors that are perpendicular to the surface and span nearly parallel faces of

the spacer layer's bulk Fermi surface. Stiles¹⁰ used a tight-binding fit to a local-density approximation of the Au band structure to compute coupling periods of 2.50 and 9.36 layers. Bruno and Chappert¹¹ used a nearly-free-electron fit to de Haas-van Alphen and cyclotron resonance measurements of Fermi surface extremals and predicted coupling periods of 2.51 and 8.60 layers for Au(100). Both calculations are in good agreement with our measured Au coupling periods of 2.48 ± 0.05 and 8.6 ± 0.3 layers, although the Bruno and Chappert calculation matches the long period better. The general agreement between our measurements and these theories further supports the hypothesis that the oscillatory exchange coupling periods in atomically well-ordered materials are determined by Fermi surface spanning vectors.

ACKNOWLEDGMENTS

We wish to thank M. D. Stiles for many helpful discussions. The whiskers were grown at Simon Fraser University under an operating grant from the National Science and Engineering Research Council of Canada. This work is supported by the Office of Technology Administration of the Department of Commerce and by the Office of Naval Research.

¹Y. Wang, P. M. Levy, and J. L. Fry, *Phys. Rev. Lett.* **65**, 2732 (1990).

²J. Unguris, R. J. Celotta, and D. T. Pierce, *Phys. Rev. Lett.* **67**, 140 (1991).

³D. T. Pierce, J. A. Strosio, J. Unguris, and R. J. Celotta (unpublished).

⁴Z. Celinski and B. Heinrich, *J. Magn. Magn. Mater.* **99**, L25 (1991).

⁵A. Fuss, S. Demokritov, P. Grünberg, and W. Zinn, *J. Magn. Magn. Mater.* **103**, L221 (1992).

⁶J. Unguris, R. J. Celotta, and D. T. Pierce, *J. Magn. Magn. Mater.* **127**, 205 (1993).

⁷J. A. Strosio, D. T. Pierce, and R. A. Dragoset, *Phys. Rev. Lett.* **70**, 3615 (1993).

⁸Y. Kuk, P. J. Silverman, and F. M. Chua, *J. Microsc.* **152**, 449 (1988).

⁹M. Ruhrig, R. Schafer, A. Hubert, R. Mosler, J. A. Wolf, S. Demokritov, and P. Grünberg, *Phys. Status Solidi A* **125**, 635 (1991).

¹⁰M. D. Stiles, *Phys. Rev. B* **48**, 7238 (1993).

¹¹P. Bruno and C. Chappert, *Phys. Rev. Lett.* **67**, 1602 (1991).